Supramolecular Rotor and Translator at Work: On-Surface Movement of Single Atoms

Robin Ohmann,[†,#] Jörg Meyer,[†] Anja Nickel,[†] Jorge Echeverria,[‡] Maricarmen Grisolia,[‡] Christian Joachim,[‡,§] Francesca Moresco,[*,†] and Gianaurelio Cuniberti[†,∥]

[†]Institute for Materials Science, Max Bergmann Center of Biomaterials, and Center for Advancing Electronics Dresden, and [∥]Dresden Center for Computational Materials Science (DCCMS), TU Dresden, 01062 Dresden, Germany, [‡]GNS & MANA Satellite, CEMES, CNRS, 29 Rue J. Marvig, 31055 Toulouse Cedex, France, and [§]International Center for Materials Nanoarchitectonics (MANA), National Institute for Materials Science (NIMS), 1-1 Namiki, Tsukuba, Ibaraki 305-0044, Japan
[#]Present address: Energy Materials and Surface Sciences Unit (EMSS), Okinawa Institute of Science and Technology Graduate University (OIST), 1919-1 Tancha, Onna-son, Okinawa 904-0495, Japan.

ABSTRACT A supramolecular nanostructure composed of four 4-acetylbiphenyl molecules and self-assembled on Au (111) was loaded with single Au adatoms and studied by scanning tunneling microscopy at low temperature. By applying voltage pulses to the supramolecular structure, the loaded Au atoms can be rotated and translated in a controlled manner. The manipulation of the gold adatoms is driven neither by mechanical interaction nor by direct electronic excitation. At the electronic resonance and driven by the tunneling current intensity, the supramolecular nanostructure performs a small amount of work of about 8×10^{-21} J, while transporting the single Au atom from one adsorption site to the next. Using the measured average excitation time necessary to induce the movement, we determine the mechanical motive power of the device, yielding about 3×10^{-21} W.

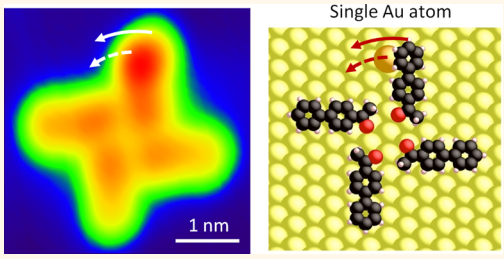

KEYWORDS: single-atom movement · supramolecular structures · voltage pulses · scanning tunneling microscopy

Conversion of electrical, chemical, or thermal energy into mechanical energy is commonly observed in nature and employed in technology in order to generate mechanical movement. For example, macromolecular protein motors[1] have been largely studied *in vitro*, converting chemical energy into mechanical energy.[2] On a surface and 1 order of magnitude smaller in diameter, single-molecule machines,[3] rotors,[4−6] and translators[7] have been demonstrated. They convert thermal or electrical energy into mechanical energy. For example, they can rotate randomly by picking up thermal energy from a sufficiently warm surface.[5] They can be driven electronically step by step by applying a voltage pulse to the molecule itself with the apex of the scanning tunneling microscope (STM) tip.[8−11] In the latter case, the electrical energy provided by the pulse is much larger than what is required to rotate or translate a single molecule on a surface. The major part of this energy is consumed in the body of the STM tip apex and dissipated throughout the solid surface supporting the molecule. The driving force for a rotation (translation) comes in the majority of cases from the electronic energy provided by the electrons tunneling through the molecule.[12,13] While billions of electrons per second are tunneling through, the energy of one electron is typically enough to generate the movement. So far, many such systems have been demonstrated, but none have shown the deliberate rotation or translation of an attached load such as an adatom or a molecule. Attempts to move atoms or molecules with the help of another molecule have been successful. However, they rely only on the mechanical interaction with the STM tip,[14,15] or the thermal noise coming from the surface is used to carry an attached molecule.[16] When the molecule carrying the load is moved mechanically following a direct interaction with the STM tip apex,[15] a deformation of its adsorption potential energy and of its conformation results and

* Address correspondence to francesca.moresco@tu-dresden.de.

Received for review May 24, 2015 and accepted July 9, 2015.

Published online July 09, 2015
10.1021/acsnano.5b03131

contributes directly to the mechanically induced motion of the molecule and its load.

Here, we demonstrate that an electronically driven supramolecular structure can generate work by moving a load such as a single atom. We have used a windmill-shaped supramolecular nanostructure composed of four 4-acetylbiphenyl molecules that self-assemble on the Au (111) surface.[11] This supramolecular structure has been demonstrated by us to convert a bias voltage pulse in a rotation or a translation step motion by the virtue of a tunneling resonant process, giving almost total access to the molecular electronic excited states' potential energy surface describing the rotation (translation) process on a Au(111) surface. By mounting single Au adatoms on one of the molecules composing the supramolecular nanostructure and applying the same bias voltage pulse as for an unloaded one, we demonstrate here that the supramolecular nanostructure can drive itself and the Au adatom load, thus performing a small amount of work. It is important to emphasize that it is the nanostructure itself and neither the tip apex mechanics[17,18] nor the direct electronic excitations of the loaded adatoms[19] that manipulates the Au adatoms.

RESULTS AND DISCUSSION

Formation and Loading of the Supramolecular Structure with a Single Gold Atom. The supramolecular structure is formed on-surface by depositing 4-acetylbiphenyl (ABP) molecules onto the Au (111) surface. Upon adsorption, four of these molecules self-assemble into windmill-like supramolecular structures (ABP_4), randomly distributed on the surface.[11] For the load we use single Au atoms, which are obtained by gently dipping the tip of the STM into the Au (111) surface. The identity of the Au adatoms is verified by topographic and spectroscopic means.[20,21] An STM topography image of the supramolecular structure and a nearby adatom is shown in Figure 1a. All four molecules composing the nanostructure have the same apparent height.

The loading of the windmill with one Au adatom is achieved by driving the supramolecular structure with voltage pulses (see Methods for details) toward the adatom. Once it is brought sufficiently close, it is snapped with a final voltage pulse to the adatom. The resulting $AuABP_4$ complex is shown in the experimental STM image of Figure 1b. Here, the protrusion at the end of one molecular wing appears much larger than for the other three wings. The height difference is about 1 Å (see line profiles in Figure 1c). The maximum is located at the outer phenyl ring of the ABP molecule where the Au atom is located. The attachment of a single Au atom to the inner phenyl ring is also possible (see Supporting Information). The calculated STM images of the pristine ABP_4 nanostructure and the loaded $AuABP_4$ are shown in Figure 1d,e. They were used to refine the Au binding location site and the conformation of the complex adsorbed on the Au (111) surface as presented in Figure 1g,h (see Methods for computational details). The structural refinement and the geometry optimization reveal that the preferred location of the Au adatom is slightly off-center with respect to the corresponding phenyl ring. This phenyl ring is not parallel to the surface anymore, but twisted with an angle of about 35°. Slight height differences between the molecular wings of the ABP_4 nanostructure after manipulation have been observed and can be attributed to different adsorption positions of the nanostructure with respect to the herringbone reconstruction of the Au (111) surface (see Supporting Information). The electronic properties of the three molecular wings with no adatom are not modified by the interaction of the adatom with the fourth wing. This is demonstrated by scanning tunneling spectra taken on the molecular wings without adatom, which reveal no difference compared to the pristine nanostructure.[11] This result is rationalized by the rather weak coupling (hydrogen bonding) between the wings, leaving the electronic properties of the windmill unchanged on the three wings free of Au.

Driving the Loaded Supramolecular Structure. After mounting the Au adatom on the supramolecular structure, we have studied its movement on the Au (111) surface. By applying a voltage pulse (at the same conditions as for the movement observed without the adatom[11]) on the $AuABP_4$ complex, not only the supramolecular structure but also the adatom moves in a concerted manner. Both rotational and translational movements can be achieved in this way. The movement of the structure is made possible by the resonant electronic excitation of the nanostructure that activates a specific movement.[11,22,23] The manipulation process is highly reproducible and in good agreement with the previous work done by us on the unloaded ABP_4 structures.[11] In Figure 2a and b, an example of rotational motion is shown. For a better visualization of the rotation, the difference of the images before and after the voltage pulse is shown in Figure 2c. The recorded height profile during the voltage pulse is presented in Figure 2a (bottom), showing a sudden change, at which point the movement happens. The time until the jump occurs is the excitation time, which will be explained in detail later on. The experiment shows that the adatom can be moved by the supramolecular nanostructure without any mechanical interaction of the tip apex. At each voltage pulse, the complex and thus the adatom are rotated by either 15° or 30°. Rotations were observed clockwise as well as anticlockwise. A preferential direction cannot be assigned but is not excluded.[9,11] Similar to the movement of the pristine supramolecular nanostructure, translational movements can be observed as presented in Figure 2d–f. At each voltage pulse, the adatom is moved by the nanostructure by about 3 ± 1 Å. Such traveling length is typically on the order of one surface lattice

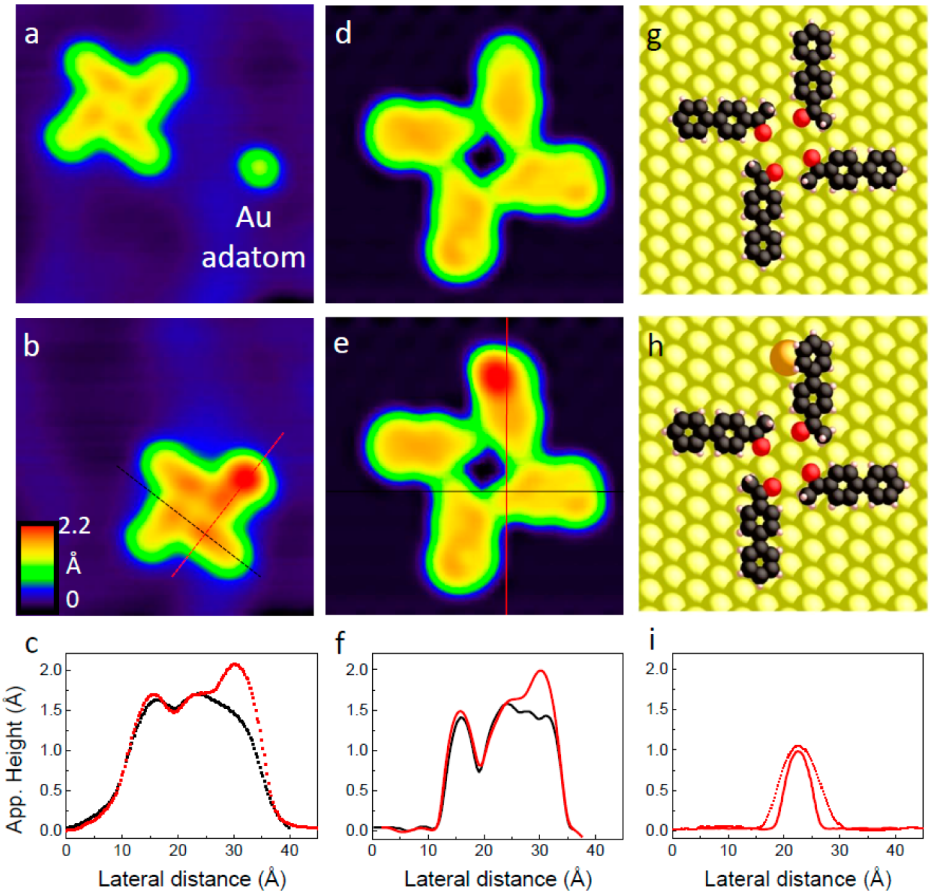

Figure 1. Characterization of the supramolecular structure before and after the loading with a Au adatom. (a) STM topography image of four 4-acetylbiphenyl molecules building ABP_4 and an isolated Au adatom on Au (111). (b) STM topography image of the same area after the attachment of the adatom to the nanostructure. (c) Experimental height profile taken at the positions marked with dashed lines in (b). (d) Calculated STM images (ESQC) corresponding to (a). (e) Calculated STM image (ESQC) corresponding to (b). (f) Calculated height profiles along the lines imprinted in (e). (g) Calculated optimized geometry of the transporter without load. (h) Calculated optimized geometry of the windmill with a Au adatom attached. (i) Height profile of the Au adatom shown in (a) (experimental data points) and calculated profile (solid line). Image sizes: (a and b) 65 × 65 Å^2, (d and e) 36 × 36 Å^2. The color code displayed in (b) applies to all images.

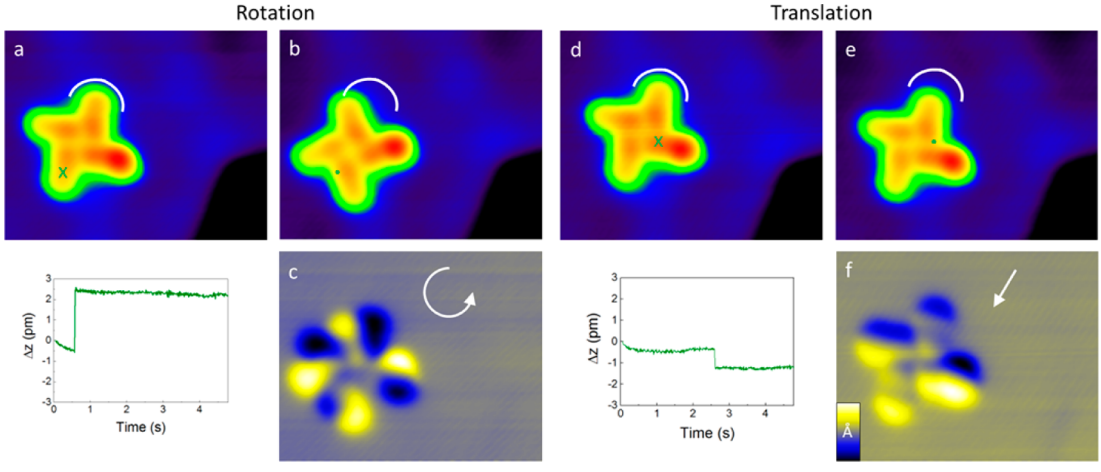

Figure 2. Rotation and translation of a single Au adatom with the electronically driven supramolecular structure. (a) STM topography image of the supramolecular structure loaded with a Au adatom. A voltage pulse is applied at the position of the green cross. The graph (bottom) reflects the time trace of the height change of the tip during the voltage pulse. (b) STM image taken after the rotation occurred. The green dot indicates the position of the voltage pulse. (c) Difference of images (a) and (b). (d–f) Same as (a)–(c), except that here a translation occurred after the voltage pulse was applied, transporting the single Au adatom in a linear movement from one adsorption site to the next. The color scale in (f) applies also to (c) and ranges from −1.3 to 1.3 Å. Image size 75 × 60 Å^2. The curved lines in (a)–(d) are a guide to the eye and show the position of one of the ABP molecules before the manipulation occurs.

constant. Which type of movement is obtained is largely determined by the polarity of the bias voltage, as outlined in detail in ref 11. For the pulse-induced manipulation of the nanostructure, the Au (111) surface reconstruction had no noticeable effect.

In contrast to the pristine supramolecular structure, we observed additional types of movements, suggesting that the adatoms can also act as pinning centers, locally increasing the adsorbate−substrate interaction.

Work Done by the Supramolecular Structure. The interaction of the ABP_4 supramolecular structure with a single Au adsorbate to form $AuABP_4$ modifies the ground-state potential energy surface (PES) of the Au adatom on the Au (111) surface (see Figure 3a−c). A potential energy "trap" is introduced by the ABP_4 nanostructure for the Au (as presented in Figure 3c) that moves along with the windmill, explaining how it can carry the Au along (see Supporting Information). When inelastically excited by the tunneling electrons during the voltage pulse and starting from one stable position on the Au (111) surface, $AuABP_4$ is undergoing its rotational motion. The fast dynamics of the rotation process occurs on the $AuABP_4$ PES first excited states. Those excited states appear in the energy range targeted by the voltage pulses. On the excited states' PES, this dynamics favors the probability of reaching another nearby minimum of the ground-state PES, avoiding the ground-state potential energy barrier by this reaction trajectory. Remarkably, the trajectory on the excited-state PES favors a rotation of the complex instead of its decomposition. This is because the trapping of the Au adatom by ABP_4 is quite strong (topology A, about 0.25 eV according to Figure 3c). As a consequence, the rotation of the complex is quite stable, as presented in Figure 3d (blue trajectory of adatom). Other possible binding sites for Au on the windmill are less stable, leading to a noncircular trajectory and to the decomposition of the complex (red in Figure 3d).

The diffusion barrier height of an isolated Au adatom on the Au (111) surface is calculated to be 247 meV (see Figure 3c and also ref 24). When the Au is loaded on the ABP_4 nanostructure, its diffusion barrier height in the windmill trap is substantially decreased to 50 meV (see Figure 3c). To overcome this barrier, the nanostructure driven by the tunneling current thus needs to develop work of at least $W_{load} = 8.0 \times 10^{-21}$ J.

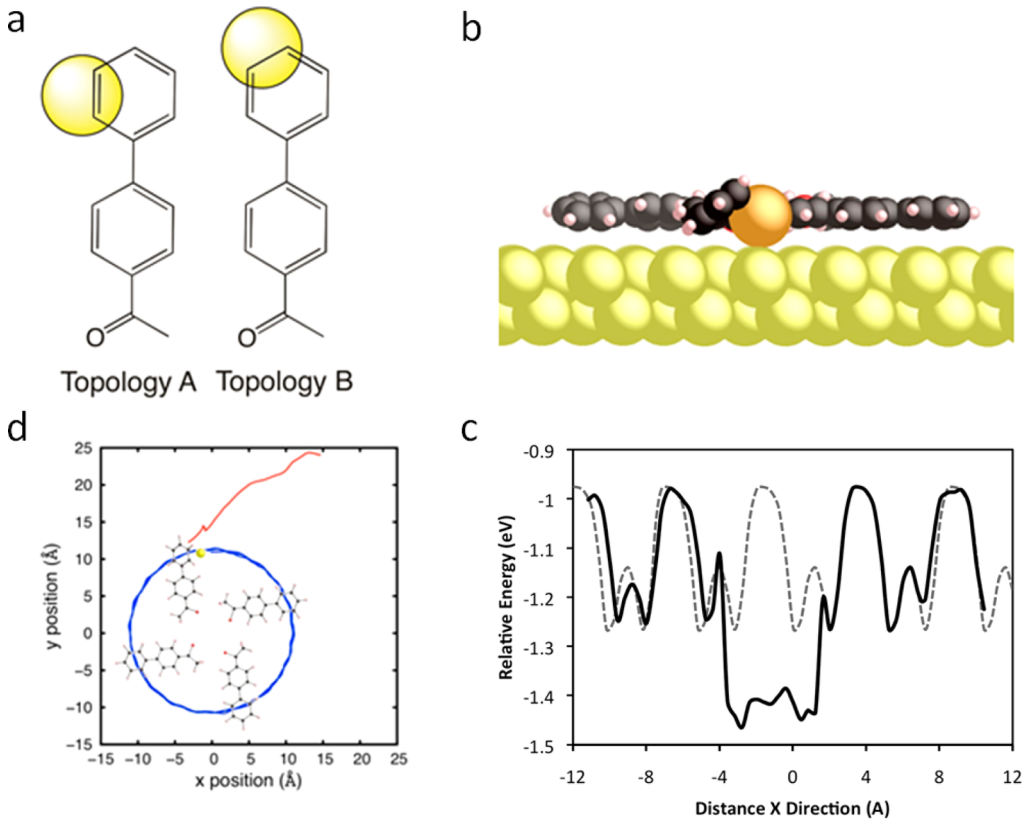

Figure 3. Simulation results of the $AuABP_4$ complex and the adatom transport. (a) Relative position of the Au adatom after geometry optimization for topologies A and B. (b) Lateral view of the windmill and the adatom with topology A on Au (111). The phenyl ring bonded to the adatom is tilted by 35° with respect to the surface. (c) Ground-state potential energy curve of a Au adatom displaced along the Au (111) surface. The dashed gray line represents the adatom displaced alone on the surface, whereas the black line results when the windmill is also present. In the center, the deep energy well is due to the complex formation between the Au adatom and the end phenyl ring of the windmill wing. The small 50 meV potential energy barrier is for the Au adatom to move from one adsorption site to the other inside this well. (d) Relative position of the Au adatom on the surface along the rotation process for topology A (blue line) and B (red line) around a rotation axis located at (0,0).

If not, there will be no motion of the complex because its load will induce a too strong opposing mechanical force, indicating that the load here is defined by the potential barrier height in its ground state and not by weight.[12]

Evaluation of the Mechanical Power. We have evaluated the mechanical power of the electron-driven supramolecular structure by dividing W_{load} by the average tunneling excitation time. The latter is obtained by averaging the measured time needed to excite a one-step rotation event, *i.e.*, the time interval between the start of the voltage pulse until a jump occurs in the recorded tip height indicating a one-step movement. We measured an average excitation time of $t_{exc} = 2.3$ s, which leads to a mechanical power of the supramolecular structure of $P_{mech} = 3.5 \times 10^{-21}$ W. The overall electrical power delivered to the STM junction during the pulse is the product of the used tunnel current (1 nA) and the voltage pulse (2.4 V), leading to $P_{elec} = 2.4 \times 10^{-09}$ W. The supramolecular structure is able to perform work W_{load} because the electrical power delivered by this pulse is orders of magnitude larger. During the pulse, a major part of the electrical power dissipates in the body of the STM tip and in the bulk of the Au sample supporting the windmill. At the STM tip apex end, the power available to the loaded windmill is only a minute portion of P_{elec}. First, the bias voltage for the pulse was chosen to be 2.4 V to access the first excited states of the complex and to trigger the inelastic tunneling effects and not to deliver this amount of electrical power to the windmill.[13] Below this electronic resonance, there are no inelastic effects and therefore no possible energy transfer to the windmill.[25] Second, the tunneling current is a measure of the number of electrons per second tunneling through the "STM tip–loaded nanostructure–Au(111) substrate" tunnel junction during a given voltage pulse. Most of the electrons are tunneling elastically without triggering any inelastic transition.[25] On the basis of the average excitation time, we calculate a quantum yield of about 7×10^{-11}. The quantum yield is the probability that an event per electron occurs and corresponds to $Y = e/I\tau$, where e is the elementary charge, I the current, and τ the average time of excitation. The electrical power for a one-electron process[11] is obtained by multiplying P_{elec} by the quantum yield, resulting in a power of 16.8×10^{-20} W. This is still above the mechanical power required for the ABP_4 nanostructure to transport its Au load and indicates

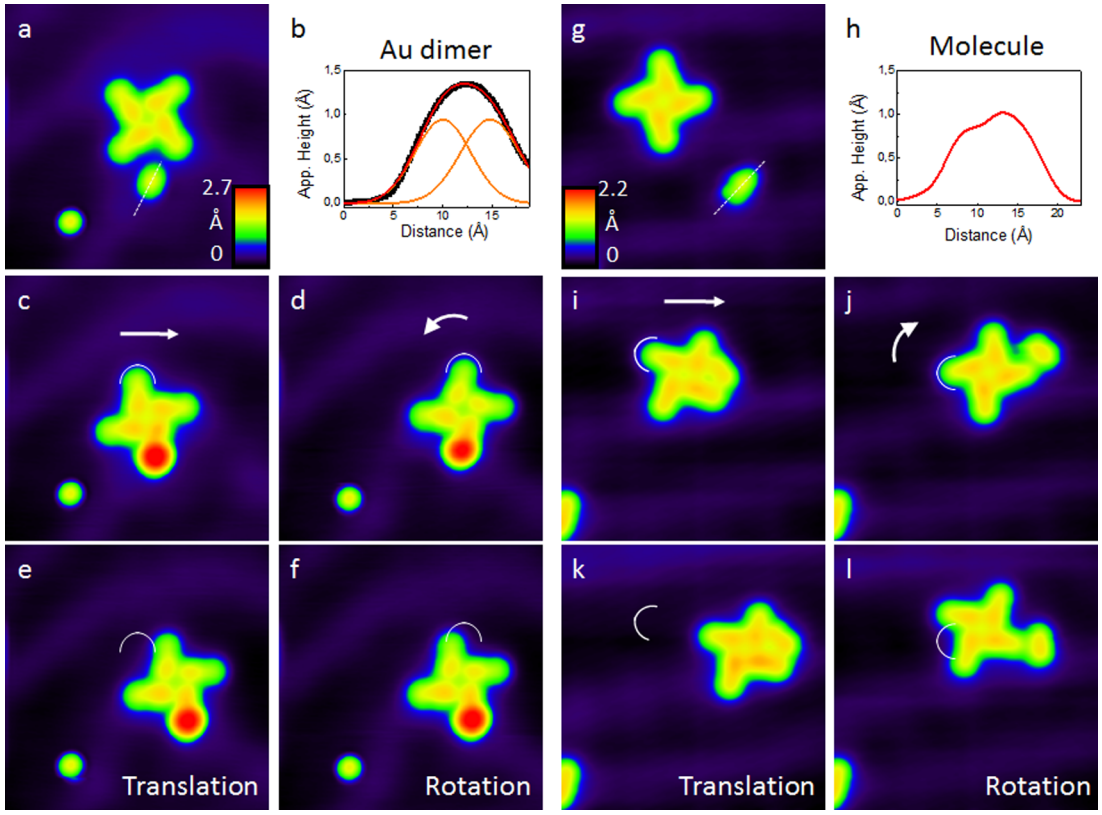

Figure 4. Rotation and translation of ABP_4 transporting a Au dimer and a molecule. Left panel: (a) STM topography image of the supramolecular structure and a Au dimer. (b) Line profile across the Au dimer (see white dashed line in (a)). Black squares are data points. The red line is a Gaussian fit composed of two Gaussians (orange) corresponding to each atom of the Au dimer. (c and d) STM images before and (e) after translation and (f) after rotation of the complex, respectively. Right panel: (g) STM topography image of ABP_4 and an additional molecular adsorbate. (h) Height profile across the molecule. (i and j) STM images before and (k and l) after electronically excited manipulation. Image sizes: 81 × 81 Å^2. The curved lines are a guide to the eye and show the position of one of the ABP molecules before the manipulation occurs.

the electrical power actually accessible to the nanostructure.

Transport of Larger Loads and Utilization for Chemical Purposes. In further experiments, an attached dimer (Au_2) was also moved using the motive power of ABP_4 (see Figure 4). Notably, in the case of a loaded molecule (an ABP molecule or its derivative), longer travel distances were observed as compared with the $AuABP_4$ complex. This can be attributed to a lower adsorbate−substrate interaction. The three examples—adatom, dimer, and molecule—show that the ABP_4 nanostructure can be loaded with different species, demonstrating its general applicability.

CONCLUSIONS

In conclusion, we have presented a nanoscale supramolecular structure that performs work. By applying voltage pulses on the nanostructure, single atoms and other species can be loaded and moved in a deliberate manner. By calculating the ground-state potential energy surface of the nanostructure with and without Au adatom load, we could determine the work needed by the molecular structure to move an atom. We conclude that a windmill structure driven by a tunneling current performs work of at least $W_{load} = 8.0 \times 10^{-21}$ J to move a gold atom on the Au(111) surface. Considering the experimentally measured average excitation time necessary to induce the movement, this work corresponds to a mechanical power of $P_{mech} = 3.5 \times 10^{-21}$ W.

On the basis of the principles shown here, other molecular electromechanical systems can be envisioned allowing future applications in the construction and integration of molecular motors and other molecular machines into more complex devices.

METHODS

The gold single-crystal surface was cleaned by repeated cycles of Ne ion sputtering and subsequent annealing at 720 K. 4-Acetylbiphenyl molecules were evaporated from a Knudsen cell at a temperature of 27 °C on a clean Au (111) surface kept at T = 50 °C. The measurements were carried out with a low-temperature scanning tunneling microscope (T = 5 K) under ultra-high-vacuum conditions (<10^{-10} mbar). After the deposition the sample was cooled to cryogenic temperatures and transferred to the STM without breaking the vacuum. For topographic imaging, either low voltages or low currents were used to ensure that no manipulation happens during scanning. Typical imaging parameters are V = 0.1 V and I = 0.1 nA. The Au adatoms were produced by gently dipping the STM tip into the gold surface.

For manipulation, the STM tip was precisely positioned on the molecules of ABP_4 and a voltage pulse between the tip and sample was applied. During the pulse, the feedback loop was kept closed and the tip height was recorded. Typical values for the voltage pulses are a bias voltage of 2.4 V, a current of 1 nA, and a time of 10 s per pulse.

The optimal molecular geometry of four ABP molecules and one Au atom on the Au(111) surface was calculated using the ASED+ semiempirical molecular mechanics technique, which is suitable for large supramolecular adsorbates.[26] STM constant-current images were calculated using ESQC (electron-scattering quantum chemistry).[27]

Conflict of Interest: The authors declare no competing financial interest.

Acknowledgment. This research was funded by the ICT-FET European Union Integrated Project AtMol and PAMS, the Deutsche Forschungsgemeinschaft (DFG), and National Science Foundation (NSF) (NSF11-568). We gratefully acknowledge support from the German Excellence Initiative via the Cluster of Excellence EXC1056 "Center for Advancing Electronics Dresden" (cfaed). The authors thank Kiran Manjunath for helping with the experimental data analysis and Carlos de Jesus Manzano Garcia for fruitful discussions.

Supporting Information Available: Further STM images and additional calculations are presented. In Figure S1, we show the attachment of a single Au atom to the inner phenyl ring. In Figure S2, additional line scans illustrating the role of the herringbone reconstruction on the apparent height of the molecule are presented. In Figure S3 we show how the supramolecular structure can also pull apart Au adatoms from a Au dimer, thus breaking a bond, and bring them back together, thus re-forming a bond. Finally, the optimized atomistic structure of $AuABP_4$ on Au(111) is discussed. The Supporting Information is available free of charge on the ACS Publications website at DOI: 10.1021/acsnano.5b03131.

REFERENCES AND NOTES

1. Soong, R. K.; Bachand, G. D.; Neves, H. P.; Olkhovets, A. G.; Craighead, H. G.; Montemagno, C. D. Powering an Inorganic Nanodevice with a Biomolecular Motor. *Science* **2000**, *290*, 1555–1558.
2. van den Heuvel, M. G. L.; Dekker, C. Motor Proteins at Work for Nanotechnology. *Science* **2007**, *317*, 333–336.
3. Joachim, C.; Rapenne, G. *Single Molecular Machines and Motors*; Springer: Berlin, 2015.
4. Michl, J.; Sykes, E. C. H. Molecular Rotors and Motors: Recent Advances and Future Challenges. *ACS Nano* **2009**, *3*, 1042–1048.
5. Gimzewski, J. K.; Joachim, C.; Schlittler, R. R.; Langlais, V.; Tang, H.; Johannsen, I. Rotation of a Single Molecule within a Supramolecular Bearing. *Science* **1998**, *281*, 531–533.
6. Fletcher, S. P.; Dumur, F.; Pollard, M. M.; Feringa, B. L. A Reversible, Unidirectional Molecular Rotary Motor Driven by Chemical Energy. *Science* **2005**, *310*, 80–82.
7. Kudernac, T.; Ruangsupapichat, N.; Parschau, M.; Macia, B.; Katsonis, N.; Harutyunyan, S. R.; Ernst, K. H.; Feringa, B. L. Electrically Driven Directional Motion of a Four-Wheeled Molecule on a Metal Surface. *Nature* **2011**, *479*, 208–211.
8. Stipe, B. C.; Rezaei, M. A.; Ho, W. Inducing and Viewing the Rotational Motion of a Single Molecule. *Science* **1998**, *279*, 1907–1909.
9. Tierney, H. L.; Murphy, C. J.; Jewell, A. D.; Baber, A. E.; Iski, E. V.; Khodaverdian, H. Y.; McGuire, A. F.; Klebanov, N.; Sykes, E. C. H. Experimental Demonstration of a Single-Molecule Electric Motor. *Nat. Nanotechnol.* **2011**, *6*, 625–629.
10. Perera, U. G. E.; Ample, F.; Kersell, H.; Zhang, Y.; Vives, G.; Echeverria, J.; Grisolia, M.; Rapenne, G.; Joachim, C.; Hla, S. W. Controlled Clockwise and Anticlockwise Rotational Switching of a Molecular Motor. *Nat. Nanotechnol.* **2013**, *8*, 46–51.
11. Nickel, A.; Ohmann, R.; Meyer, J.; Grisolia, M.; Joachim, C.; Moresco, F.; Cuniberti, G. Moving Nanostructures: Pulse-Induced Positioning of Supramolecular Assemblies. *ACS Nano* **2013**, *7*, 191–197.
12. Echeverria, J.; Monturet, S.; Joachim, C. One-Way Rotation of a Molecule-Rotor Driven by a Shot Noise. *Nanoscale* **2014**, *6*, 2793–2799.

13. Joachim, C.; Ratner, M. A. Molecular Electronics: Some Views on Transport Junctions and Beyond. *Proc. Natl. Acad. Sci. U. S. A.* **2005**, *102*, 8801–8808.
14. Yamachika, R.; Grobis, M.; Wachowiak, A.; Crommie, M. F. Controlled Atomic Doping of a Single C-60 Molecule. *Science* **2004**, *304*, 281–284.
15. Gross, L.; Rieder, K. H.; Moresco, F.; Stojkovic, S. M.; Gourdon, A.; Joachim, C. Trapping and Moving Metal Atoms with a Six-Leg Molecule. *Nat. Mater.* **2005**, *4*, 892–895.
16. Wong, K. L.; Pawin, G.; Kwon, K. Y.; Lin, X.; Jiao, T.; Solanki, U.; Fawcett, R. H. J.; Bartels, L.; Stolbov, S.; Rahman, T. S. A Molecule Carrier. *Science* **2007**, *315*, 1391–1393.
17. Eigler, D. M.; Schweizer, E. K. Positioning Single Atoms with a Scanning Tunneling Microscope. *Nature* **1990**, *344*, 524–526.
18. Ternes, M.; Lutz, C. P.; Hirjibehedin, C. F.; Giessibl, F. J.; Heinrich, A. J. The Force Needed to Move an Atom on a Surface. *Science* **2008**, *319*, 1066–1069.
19. Morgenstern, K.; Lorente, N.; Rieder, K. H. Controlled Manipulation of Single Atoms and Small Molecules Using the Scanning Tunnelling Microscope. *Phys. Status Solidi B* **2013**, *250*, 1671–1751.
20. Soe, W.-H.; Manzano, C.; Renaud, N.; de Mendoza, P.; De Sarkar, A.; Ample, F.; Hliwa, M.; Echavarren, A. M.; Chandrasekhar, N.; Joachim, C. Manipulating Molecular Quantum States with Classical Metal Atom Inputs: Demonstration of a Single Molecule nor Logic Gate. *ACS Nano* **2011**, *5*, 1436–1440.
21. Limot, L.; Pehlke, E.; Kröger, J.; Berndt, R. Surface-State Localization at Adatoms. *Phys. Rev. Lett.* **2005**, *94*, 036805.
22. Lastapis, M.; Martin, M.; Riedel, D.; Hellner, L.; Comtet, G.; Dujardin, G. Picometer-Scale Electronic Control of Molecular Dynamics inside a Single Molecule. *Science* **2005**, *308*, 1000–1003.
23. Swart, I.; Sonnleitner, T.; Niedenführ, J.; Repp, J. Controlled Lateral Manipulation of Molecules on Insulating Films by Stm. *Nano Lett.* **2012**, *12*, 1070–1074.
24. Boisvert, G.; Lewis, L. J.; Puska, M. J.; Nieminen, R. M. Energetics of Diffusion on the (100) and (111) Surfaces of Ag, Au, and Ir from First Principles. *Phys. Rev. B: Condens. Matter Mater. Phys.* **1995**, *52*, 9078–9085.
25. Monturet, S.; Kepenekian, M.; Robles, R.; Lorente, N.; Joachim, C. Vibrational Transition Rule During a through-Bond Electron Transfer Process. *Chem. Phys. Lett.* **2013**, *567*, 1–5.
26. Yu, M.; et al. Supramolecular Architectures on Surfaces Formed through Hydrogen Bonding Optimized in Three Dimensions. *ACS Nano* **2010**, *4*, 4097–4109.
27. Sautet, P.; Joachim, C. Calculation of the Benzene on Rhodium STM Images. *Chem. Phys. Lett.* **1991**, *185*, 23–30.